Supplementary Information

Naphthalene containing amino-ether macrocycle based Cu(II) templated [2]pseudorotaxanes and OFF/ON fluorescence switching *via* axle substitution

Somnath Bej and Pradyut Ghosh*

School of Chemical Sciences, Indian Association for the Cultivation of Science, 2A & 2B Raja S. C. Mullick Road, Kolkata 700032, India.E-mail: icpg@iacs.res.in

---

List of contents

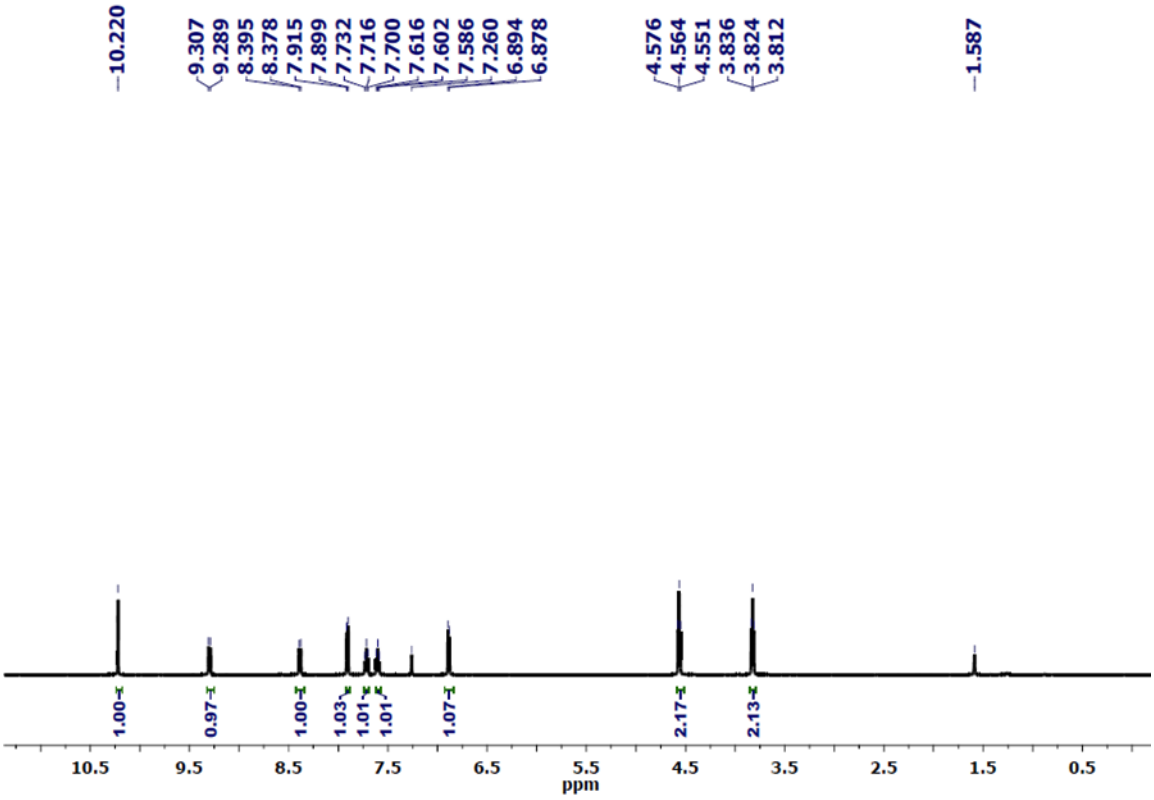

Figure 1S: ^{1}H-NMR spectrum of compound **A** in $CDCl_3$ (500 MHz) at 298 K.

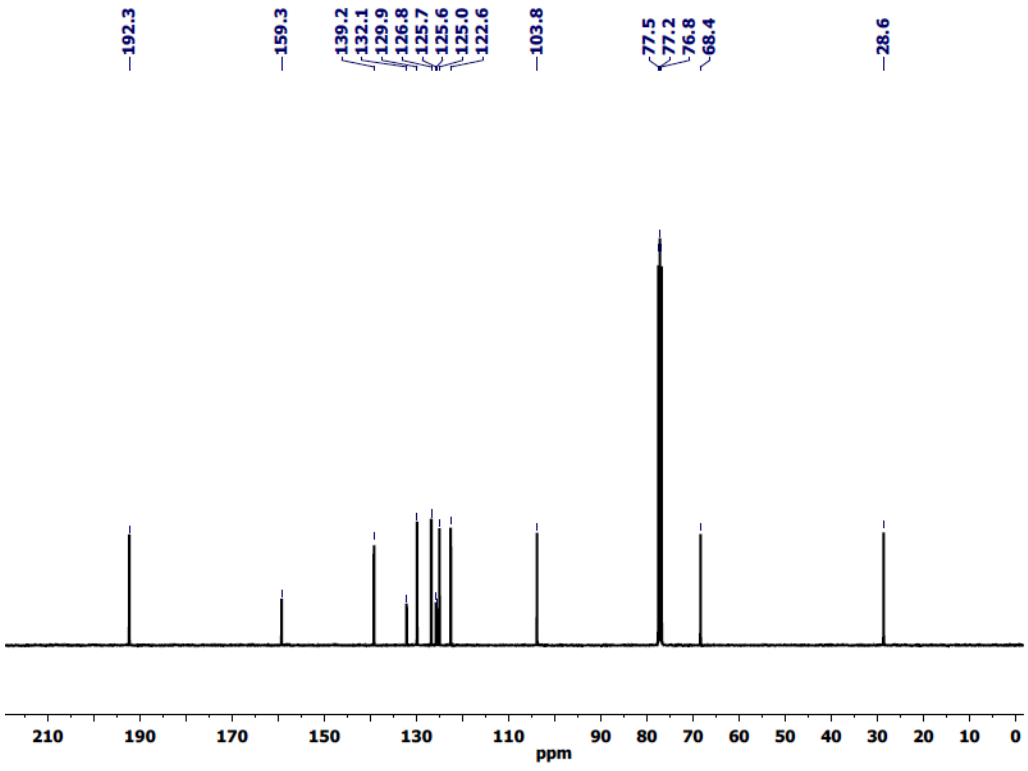

Figure 2S: ^{13}C-NMR spectrum of compound **A** in $CDCl_3$ (100 MHz) at 298 K.

.

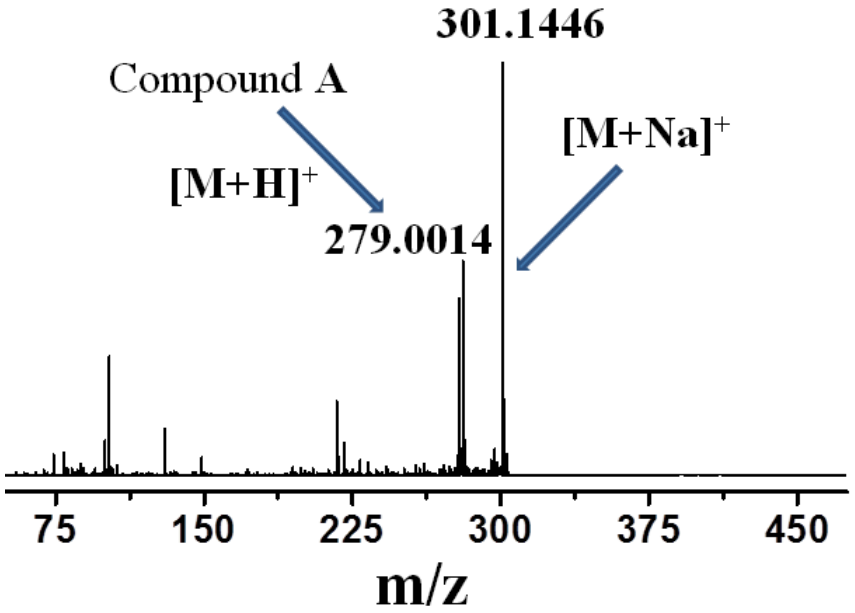

Figure 3S: ESI-MS(+ve) spectrum of compound **A.**

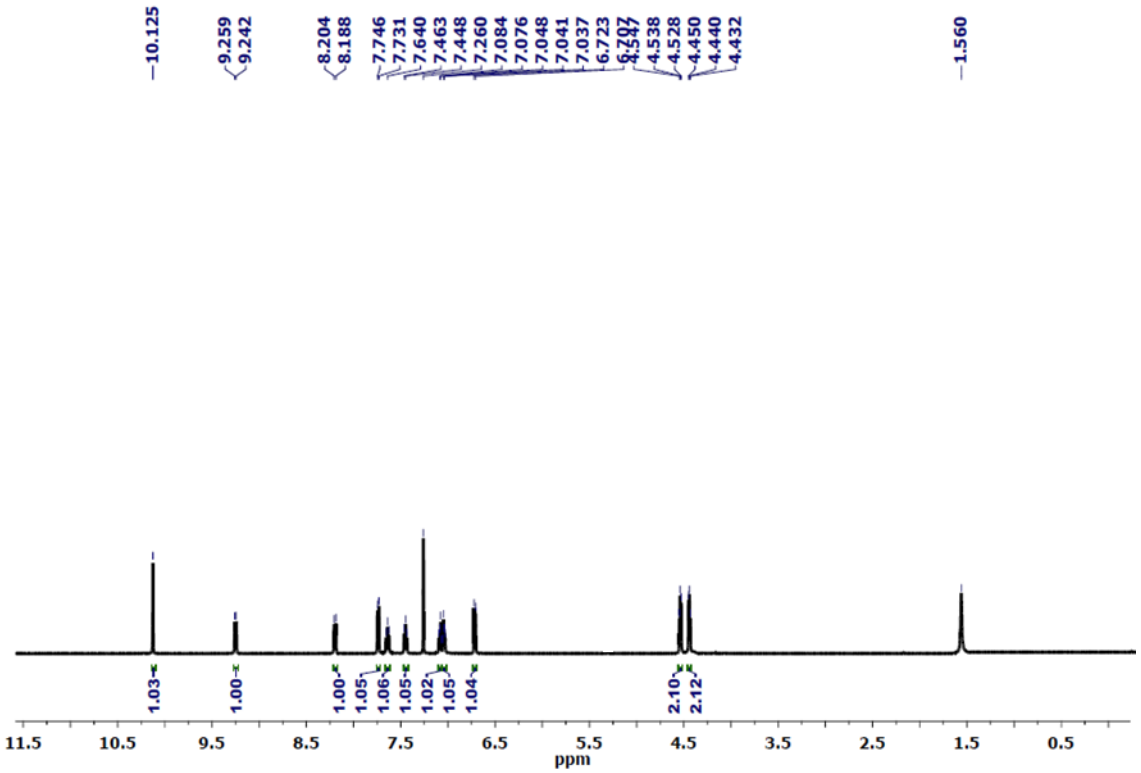

Figure 4S: ^{1}H-NMR spectrum of compound **B** in $CDCl_3$ (500 MHz) at 298 K.

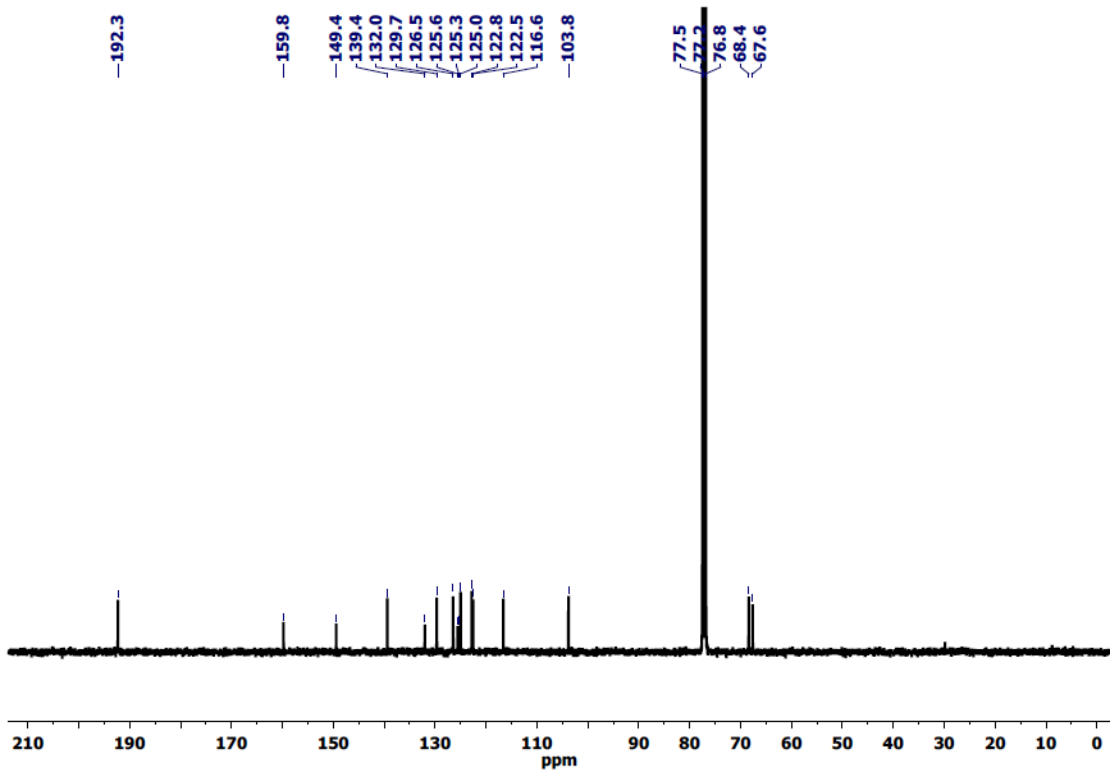

Figure 5S: ^{13}C-NMR spectrum of compound **B** in $CDCl_3$ (100 MHz) at 298 K.

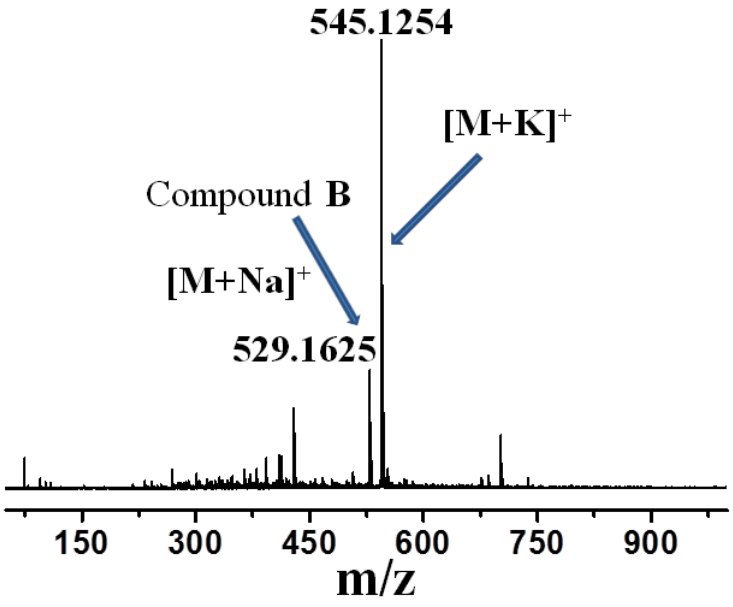

Figure 6S: ESI-MS (+ve) spectrum of compound **B.**

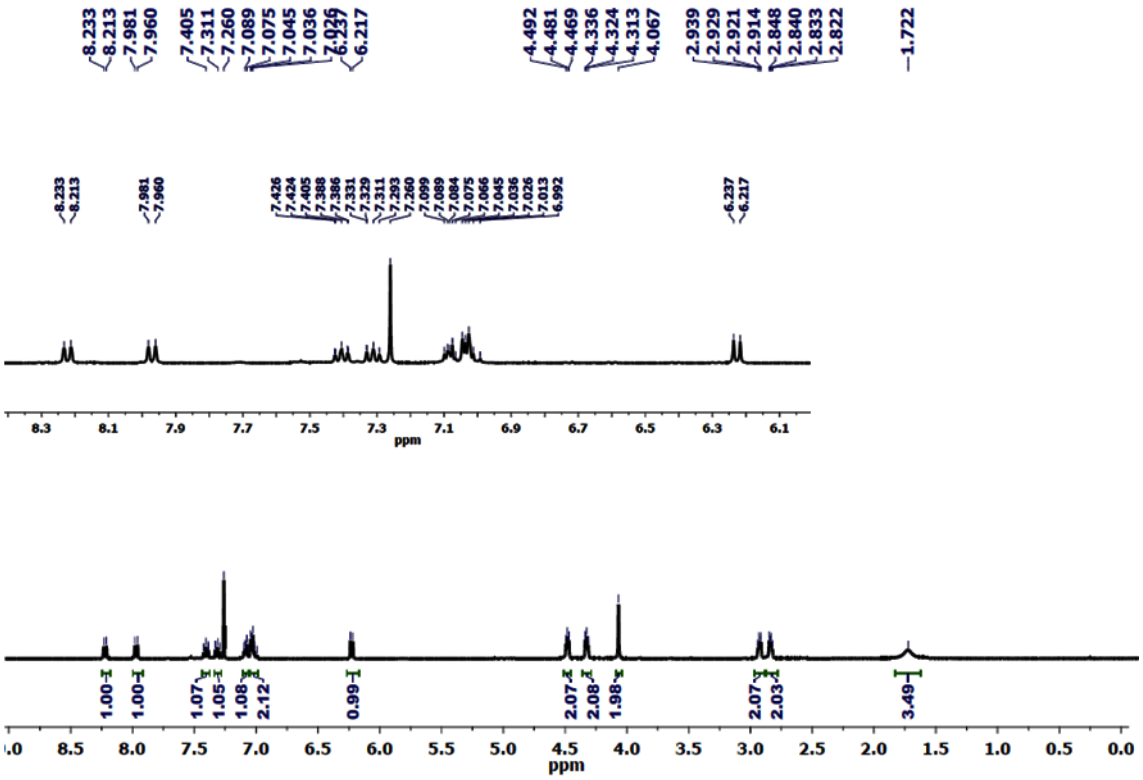

Figure 7S: ^{1}H-NMR spectrum of **NaphMC** in $CDCl_3$ (400 MHz) at 298 K.

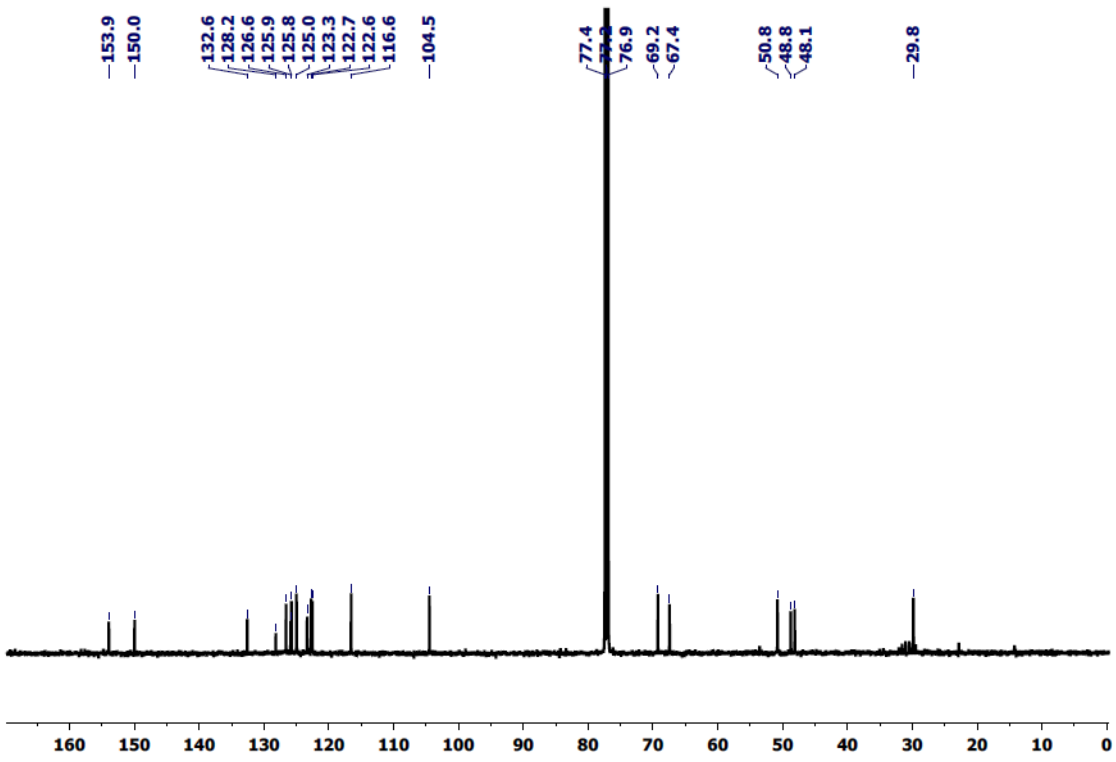

Figure 8S:^{13}C-NMR spectrum of **NaphMC** in $CDCl_3$ (125 MHz) at 298 K.

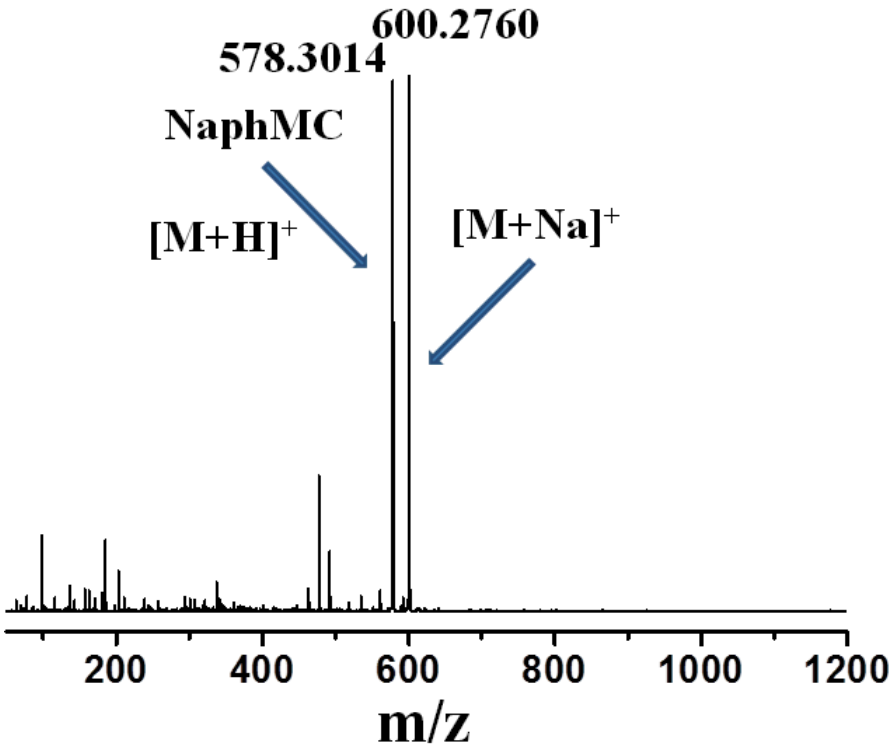

Figure 9S: ESI-MS(+ve) spectrum of **NaphMC.**

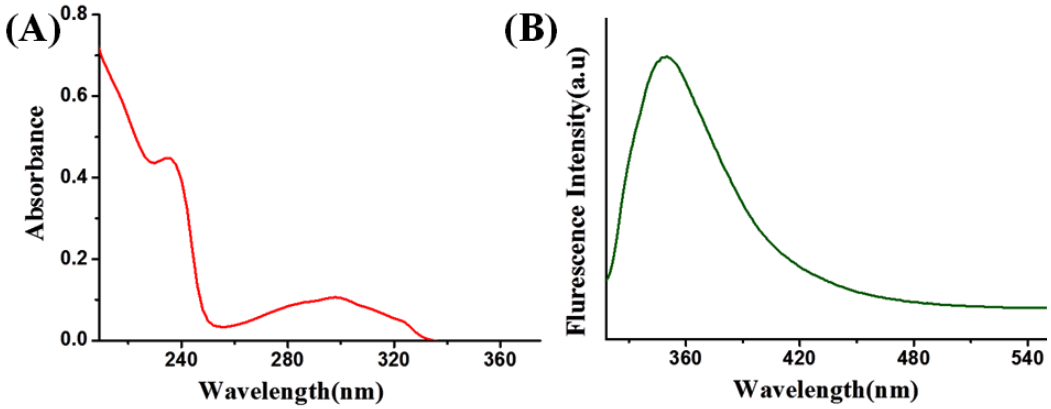

Figure 10S: (A) UV/Vis and (B) emission spectra of **NaphMC**(1 X 10^{-5} M) in dry THF at 298 K, λ_{exc}= 300 nm.

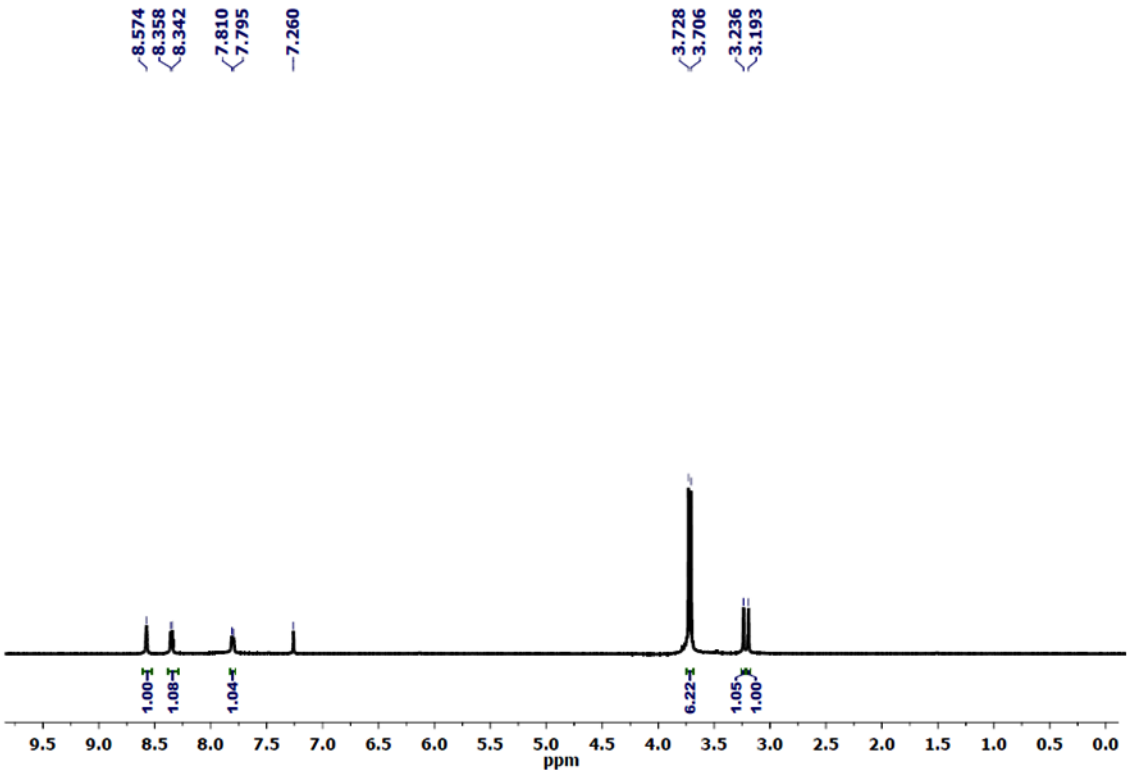

Figure 11S:[1]H-NMR spectrum of compound **D** in $CDCl_3$ (500 MHz) at 298 K.

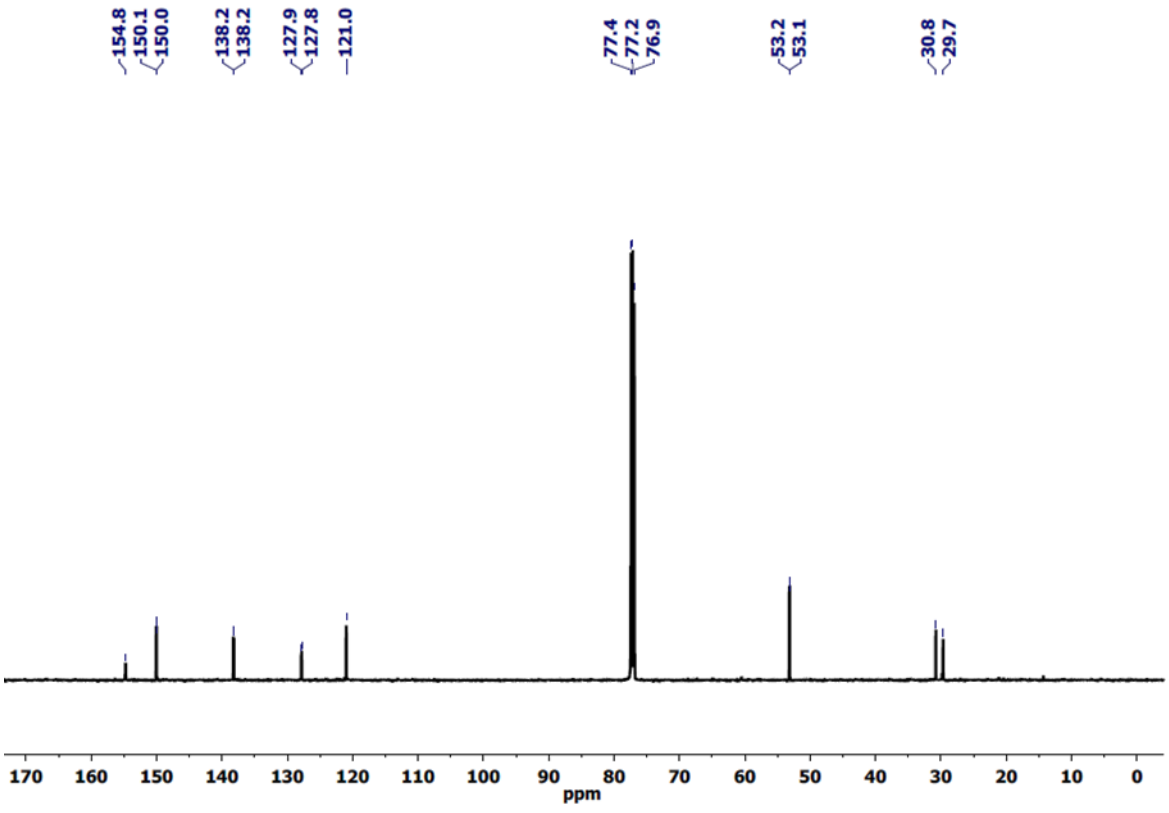

Figure 12S:[13]C-NMR spectrum of compound **D** in $CDCl_3$ (125 MHz) at 298 K.

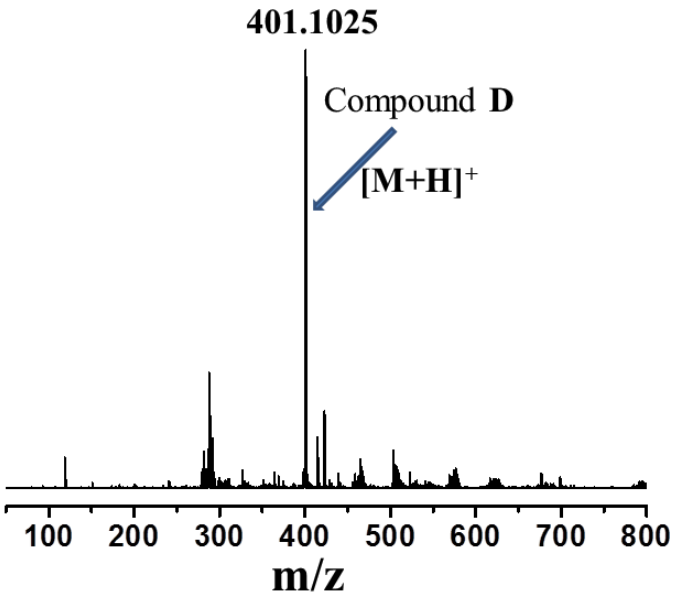

Figure 13S: ESI-MS(+ve) spectrum of compound **D.**

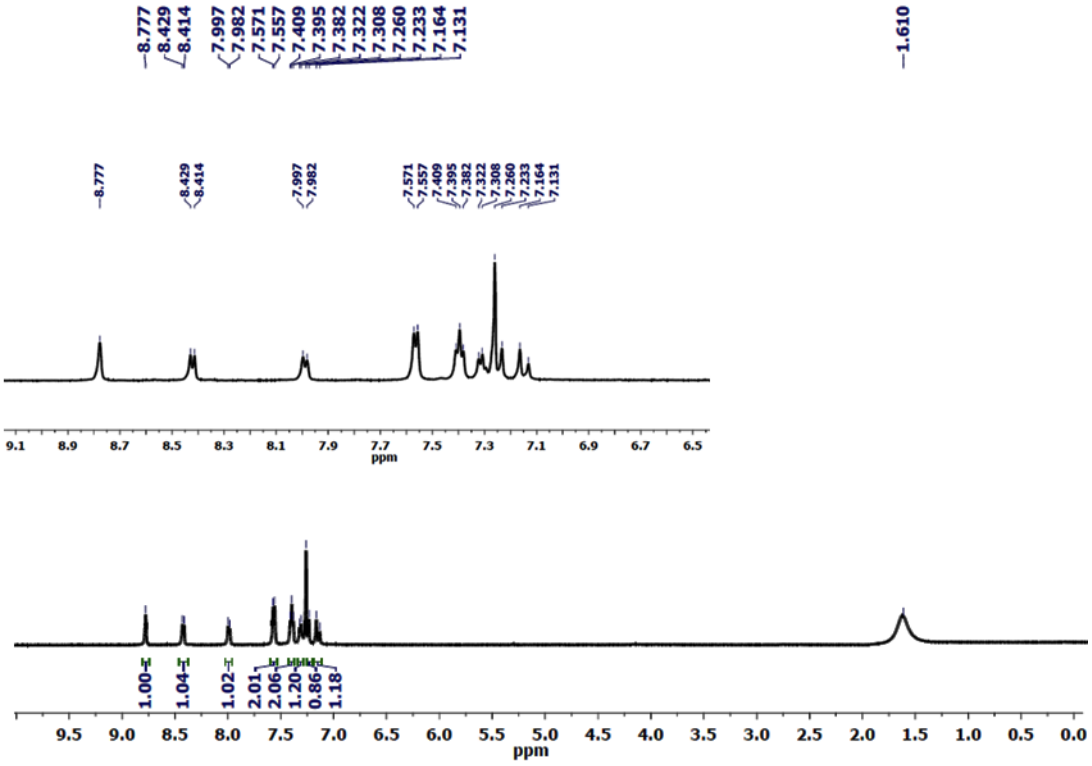

Figure 14S:[1]H-NMR spectrum of **L3** in $CDCl_3$ (500 MHz) at 298 K.

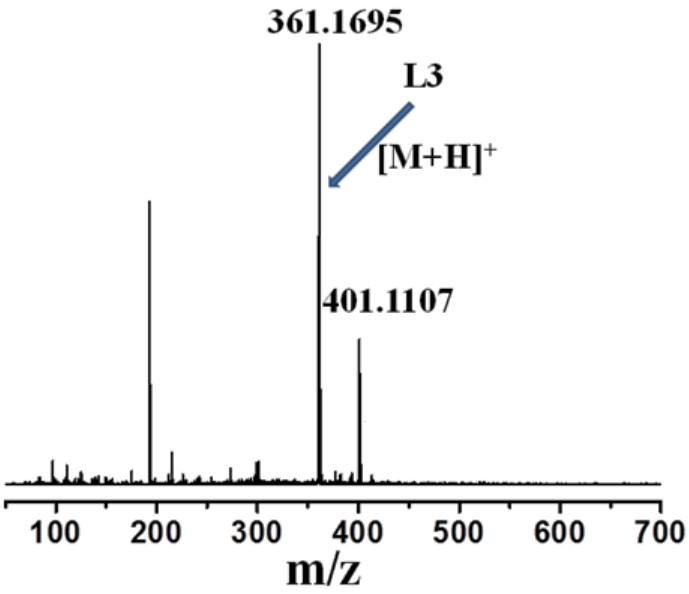

Figure 15S: ESI-MS(+ve) spectrum of **L3.**

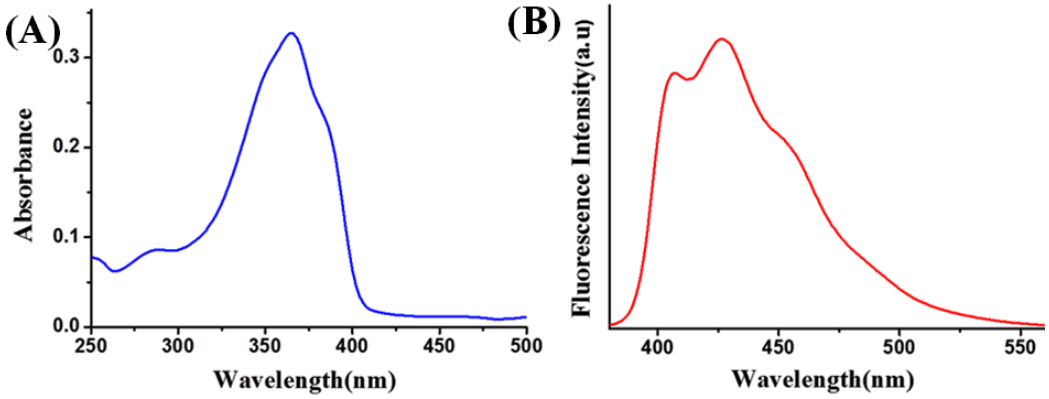

Figure 16S: (A) UV/Vis and (B) emission spectra of **L3** (1 X 10^{-5} M) in dry THF at 298 K, λ_{exc}= 362 nm.

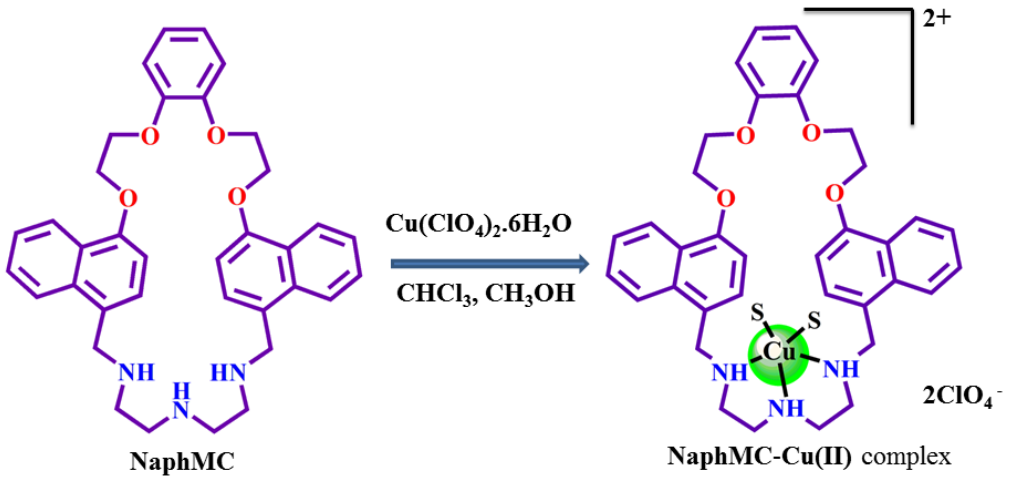

Scheme 1S. Synthetic route of the **NaphMC-Cu^{II}** complex [S= solvent molecule].

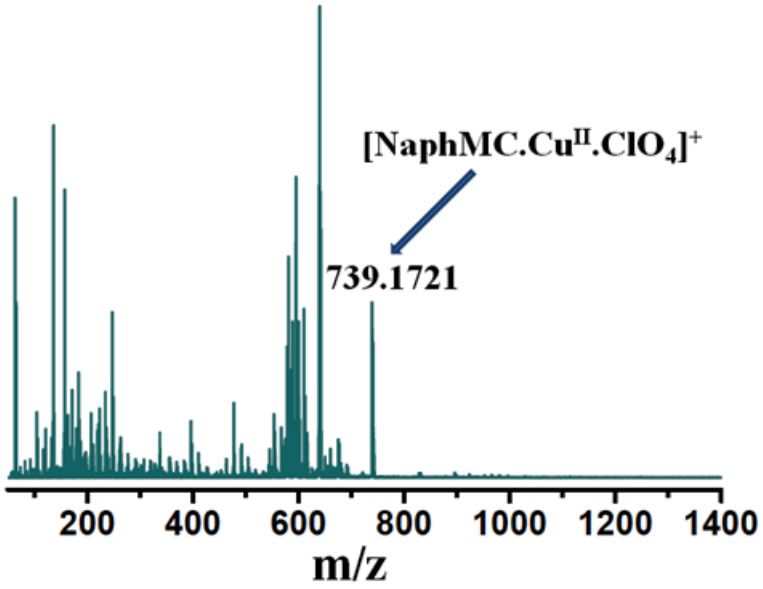

Figure 17S: ESI-MS(+ve) spectrum of **NaphMC-Cu^{II}** complex.

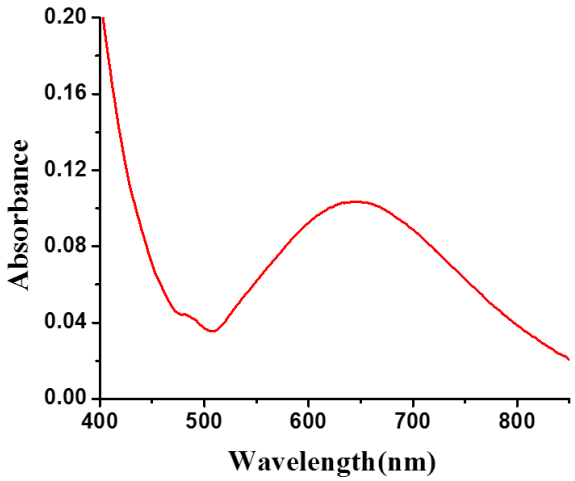

Figure 18S: Characteristic UV/Vis spectrum of **NaphMC-Cu ^{II}** complex in CH_3OH at 298K.

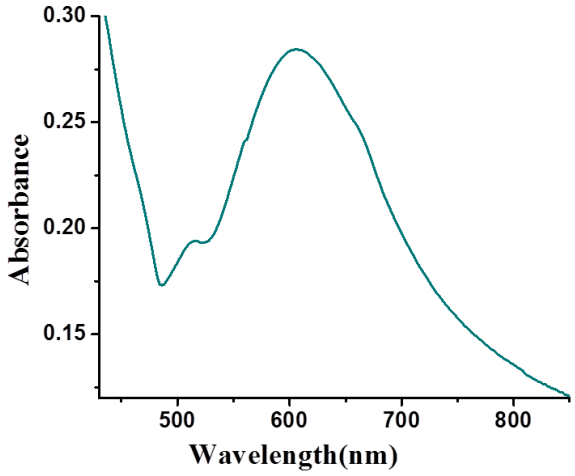

Figure 19S: Characteristic UV/Vis spectrum of **NaphMC-Cu^{II}** complex in CH_3CN at 298 K.

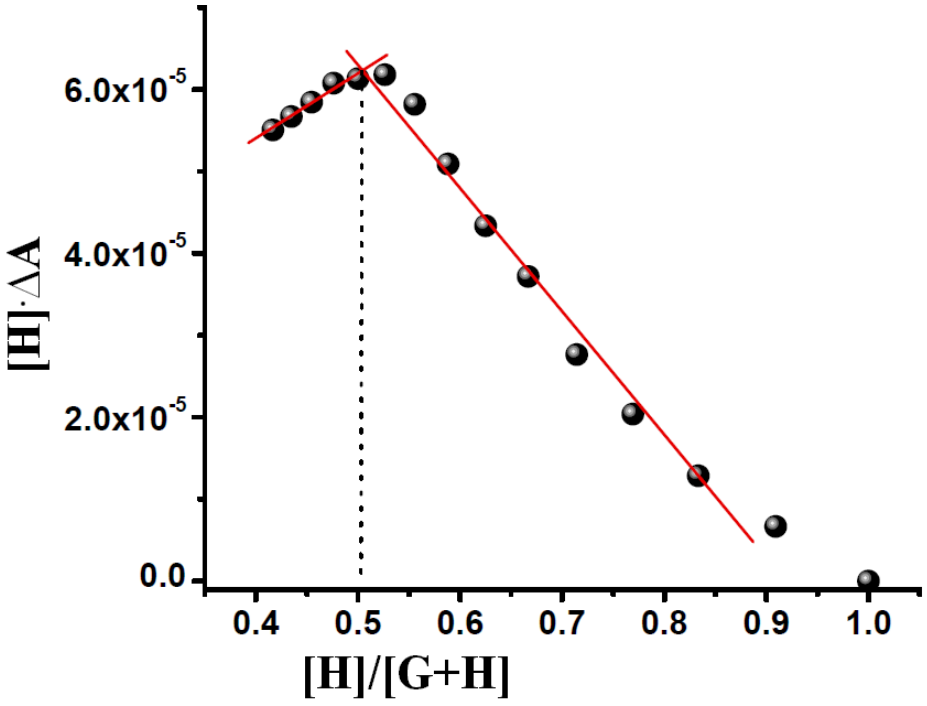

Figure 20S: Molar ratio plot from UV/Vis titration experiment between **NaphMC** with $Cu(ClO_4)_2$.

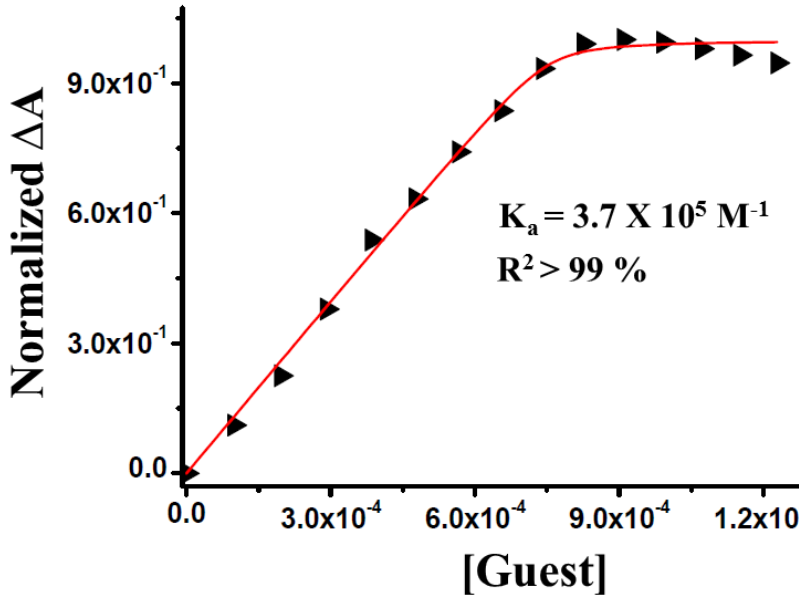

Figure21S: Nonlinear 1:1 curve fitting to determine binding constant for **NaphMC-Cu^{II}** complex from UV/Vis titration experiment in MeOH.

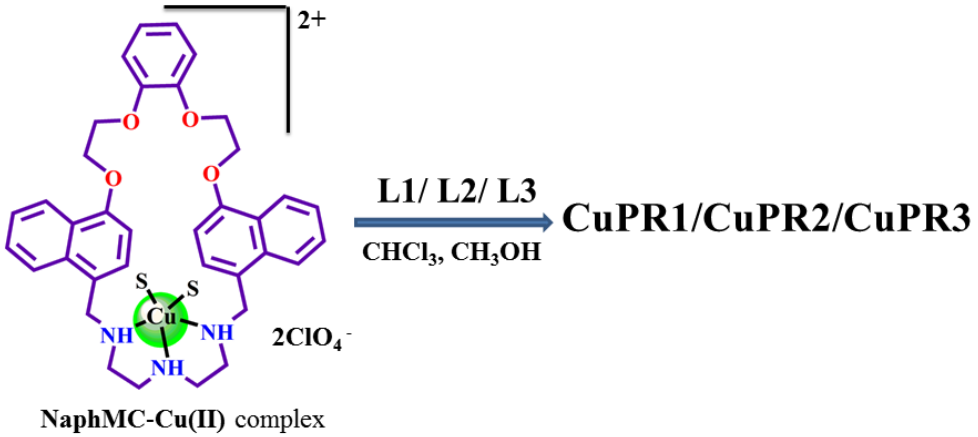

Scheme2S. Synthetic route of [2]pseudorotaxanes, **CuPR1- CuPR3.**

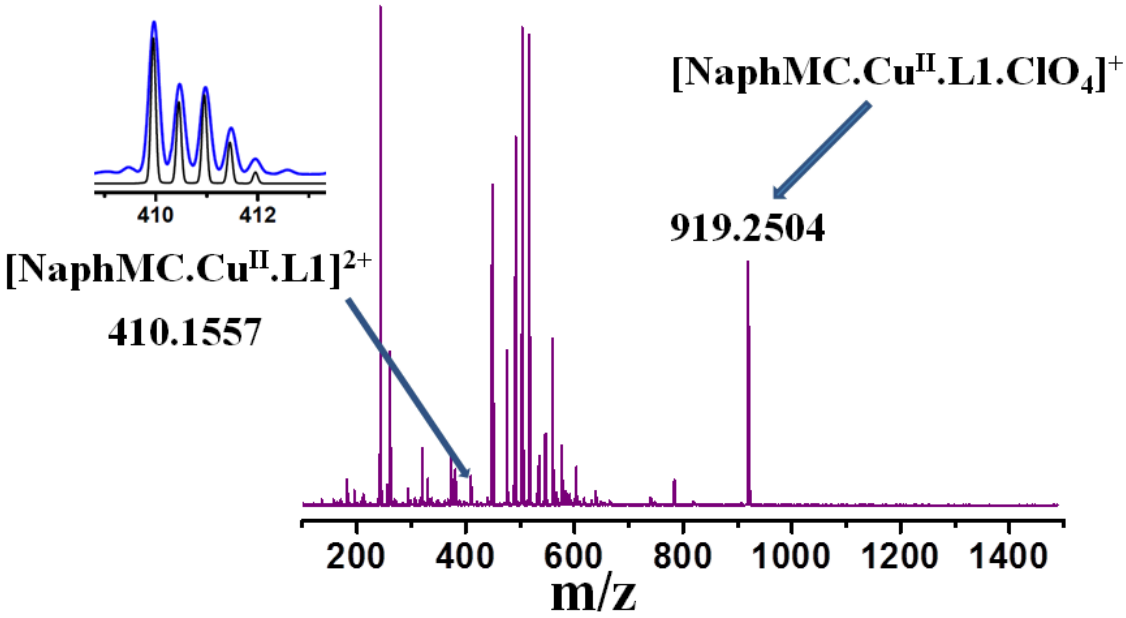

Figure22S: ESI-MS (+ve) spectrum of [2]pseudorotaxane **CuPR1** (inset shows the isotopic distribution pattern corresponding to [**NaphMC.Cu^{II}.L1**]$^{2+}$ with blue line for the experimental and black line for calculated pattern).

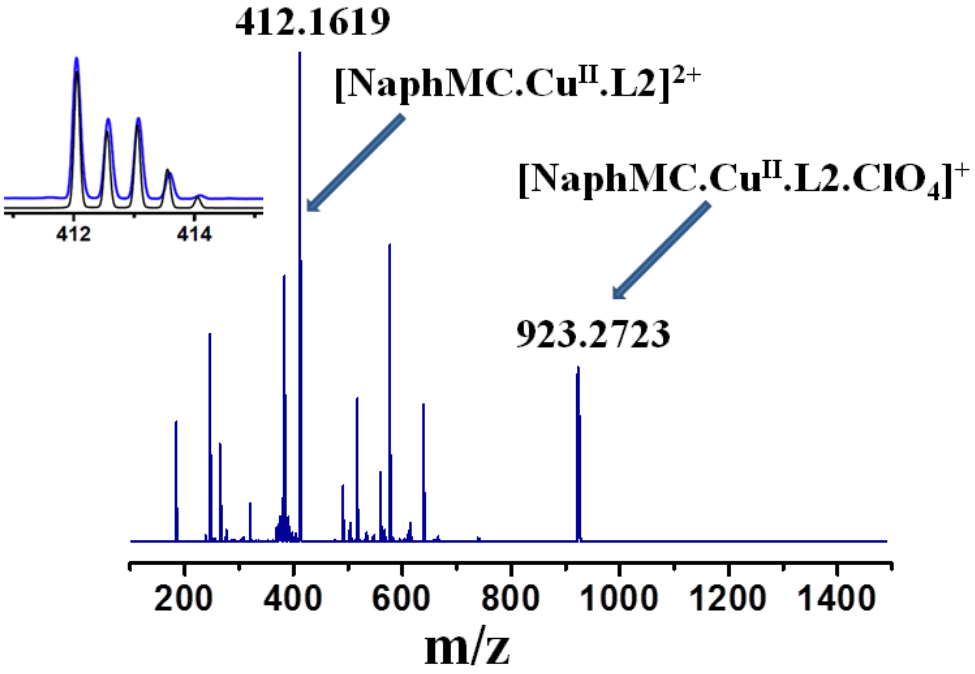

Figure 23S: ESI-MS (+ve) spectrum of [2]pseudorotaxane **CuPR2** (inset shows the isotopic distribution pattern corresponding to [**NaphMC.Cu^{II}.L2**]$^{2+}$ with blue line for the experimental and black line for calculated pattern).

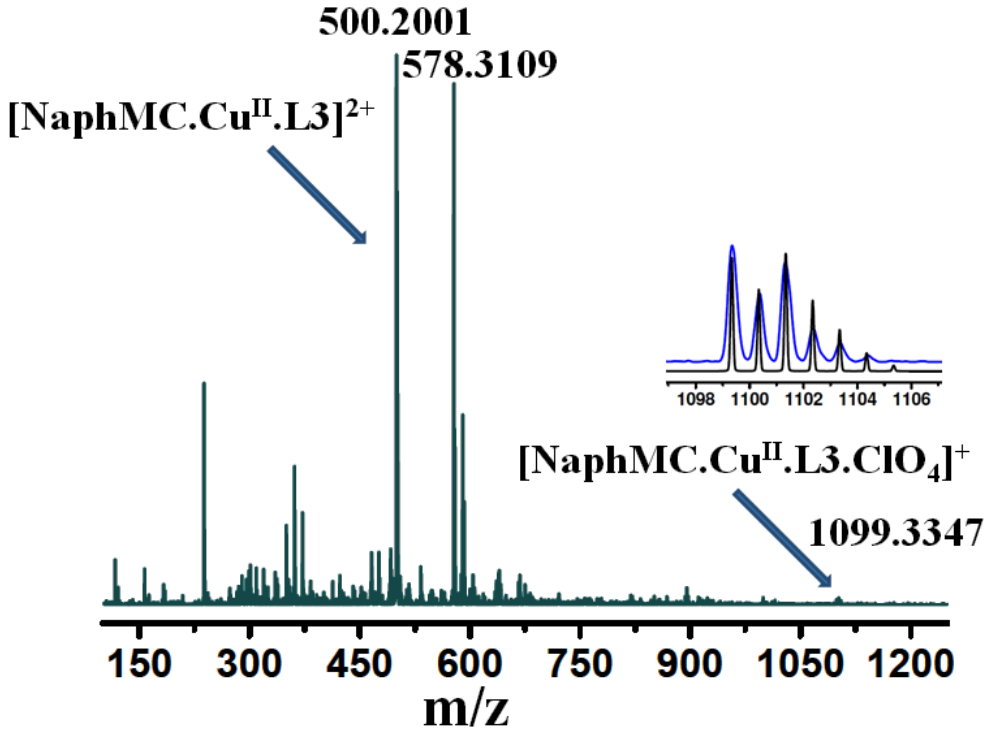

Figure 24S: ESI-MS (+ve) spectrum of [2]pseudorotaxane **CuPR3** (inset shows the isotopic distribution pattern corresponding to [**NaphMC.Cu^{II}.L3. ClO$_4$**]$^{+}$ with blue line for the experimental and black line for calculated pattern).

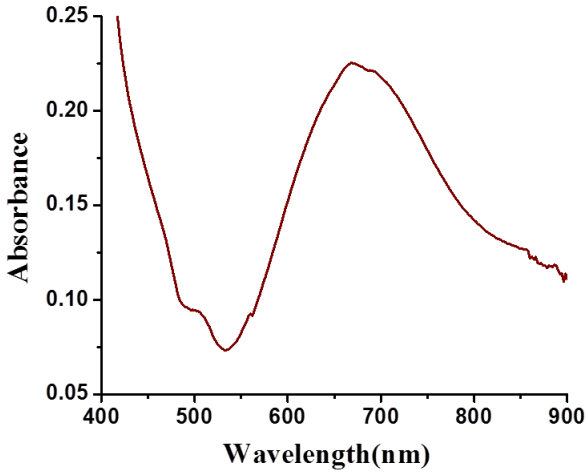

Figure 25S: Characteristic UV/Vis spectrum of **CuPR1** in CH_3CN at 298 K.

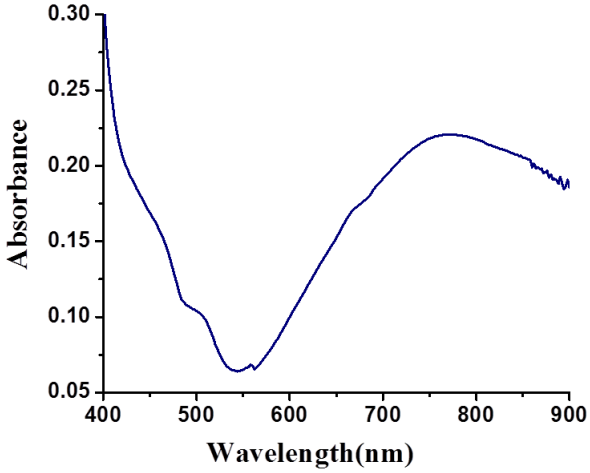

Figure 26S: Characteristic UV/Vis spectrum of **CuPR2** in CH_3CN at 298 K.

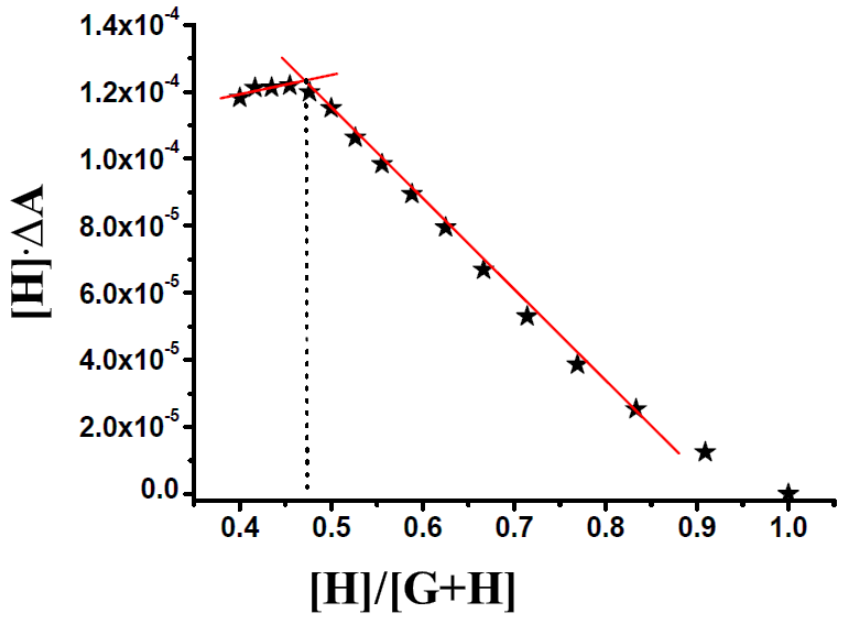

Figure 27S: Molar ratio plot from UV/Vis titration experiment between **NaphMC-Cu^{II}** with **L1.**

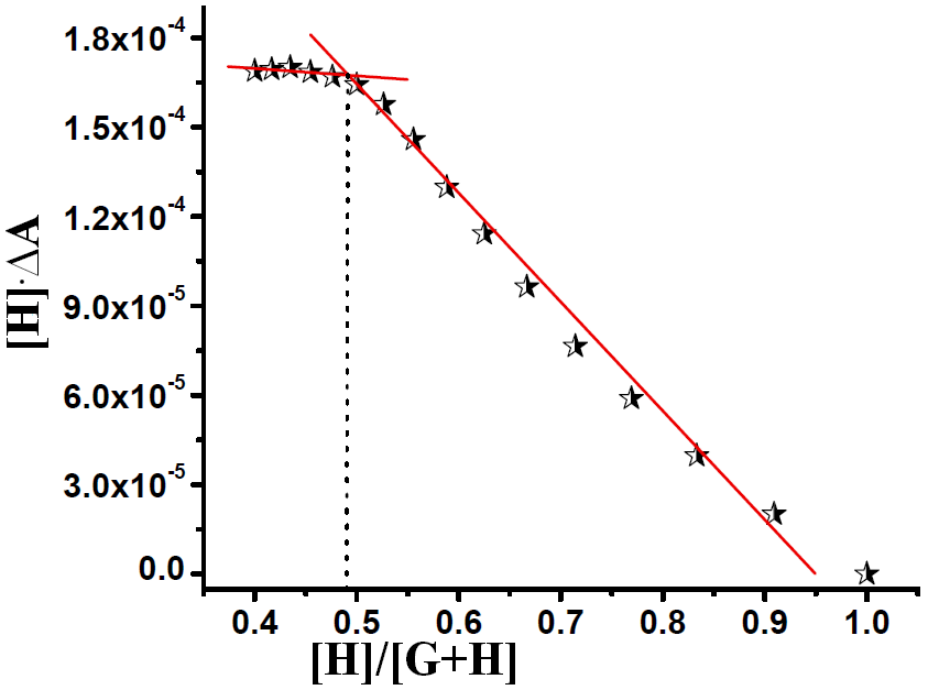

Figure 28S: Molar ratio plot from UV/Vis titration experiment between **NaphMC-Cu^{II}** with **L2.**

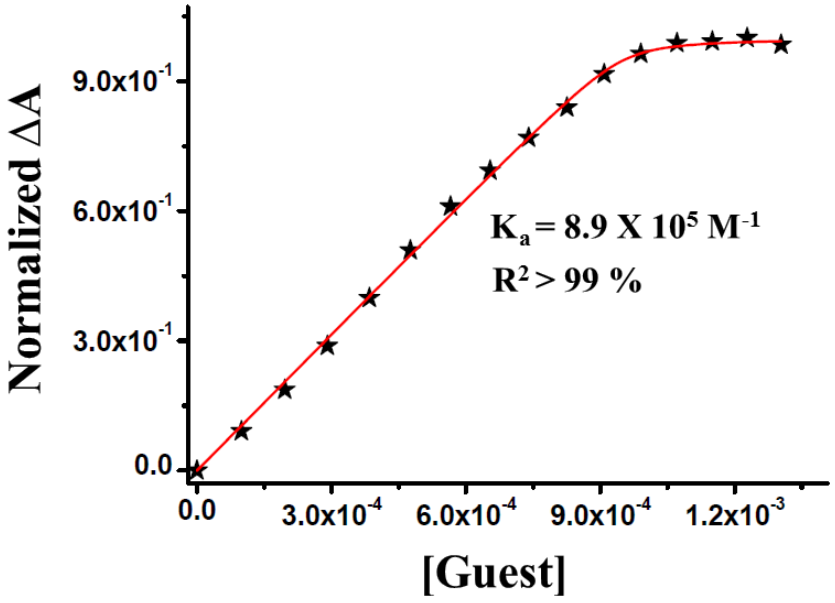

Figure 29S: Nonlinear 1:1 curve fitting plot of formation of **CuPR1** complex from UV/Vis titration experiment.

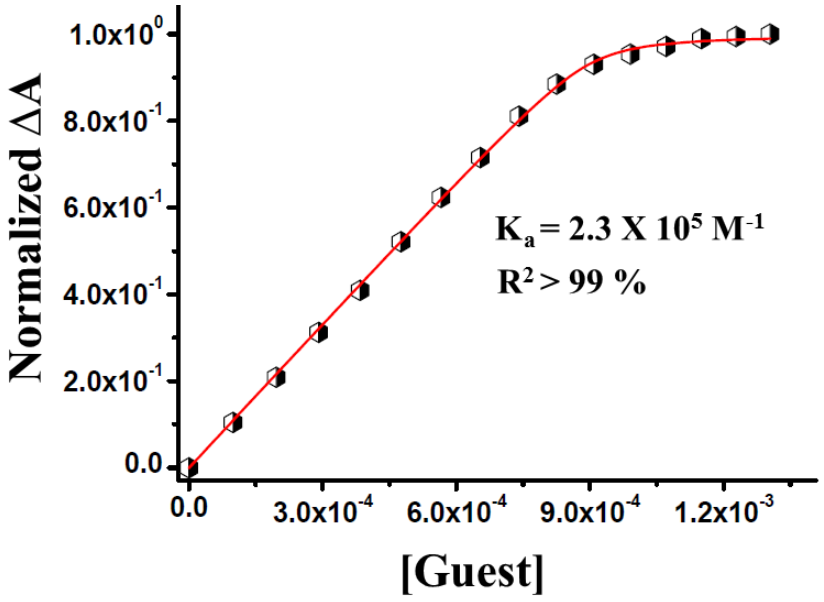

Figure 30S: Nonlinear 1:1 curve fitting plot of formation of**CuPR2** complex from UV/Vis titration experiment.

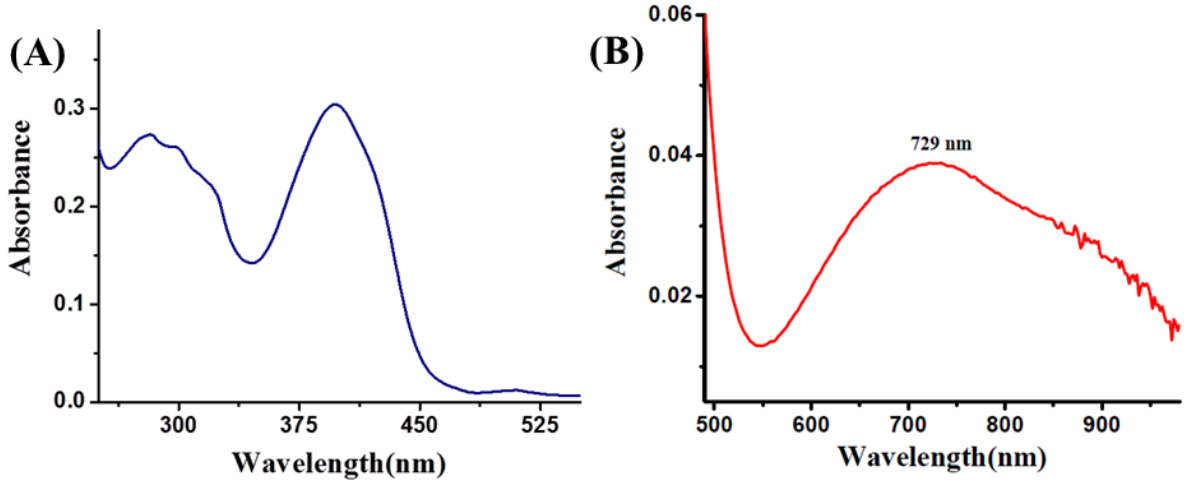

Figure 31S: Characteristic UV/Vis spectrum at 298 K (A) **CuPR3** in THF at UV region, (B) **CuPR3** at Visible region in THF.

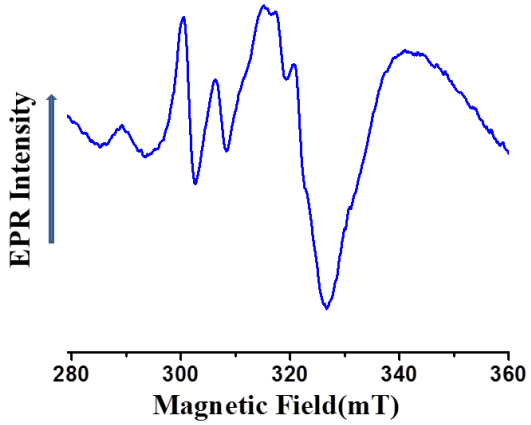

Figure 32S: EPR spectrum of **CuPR1** in DMF at 80K.

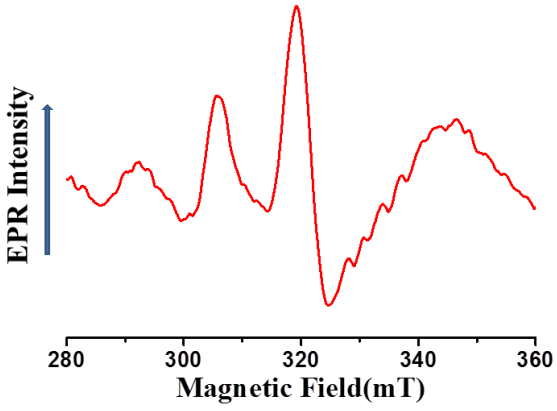

Figure 33S: EPR spectrum of **CuPR2** in DMF at 80K.

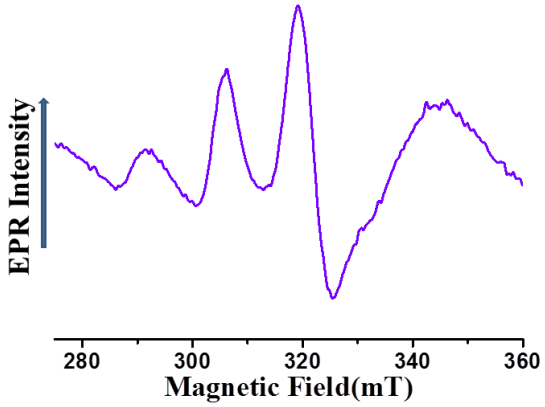

Figure 34S: EPR spectrum of **CuPR3** in DMF at 80K.

Table 1S. $g_{\|} > g_{\perp}$ values[a] of **CuPR1-CuPR3** from EPR spectra in DMF

[2]pseudorotaxane	$g_{\|}$	$g_{\perp}$
CuPR1	2.09	1.99
CuPR2	2.17	2.02
CuPR3	2.15	2.02

[a]$g_{\|}$ and $g_{\perp}$ values[2,3] from the EPR spectrum analyzed by the following equation[1]:

$$h\nu = g\beta B,$$

$$g = 71.4484\nu \text{ (in GHz)}/B \text{ (in mT)}$$

[where, ν= Microwave frequency, B= Magnetic field, β= Bohr magneton constant, h = Planck's constant].

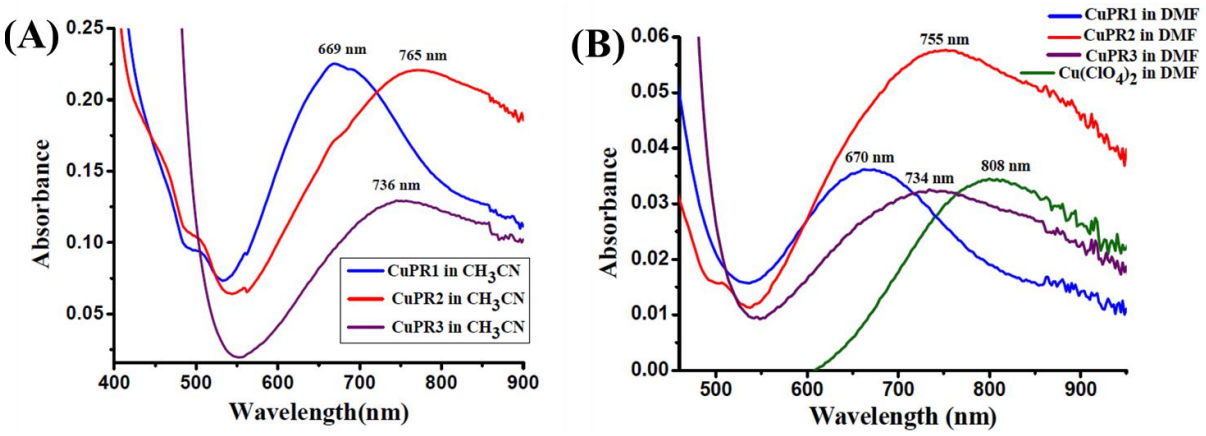

Figure 35S: Characteristic UV/Vis spectra of (A) **CuPR1**, **CuPR2** and **CuPR3** in CH_3CN and (B) **CuPR1**, **CuPR2**, **CuPR3** and **$Cu(ClO_4)_2$** in DMF medium at 298 K.

Crystallographic details of **CuPR1**and **CuPR2**

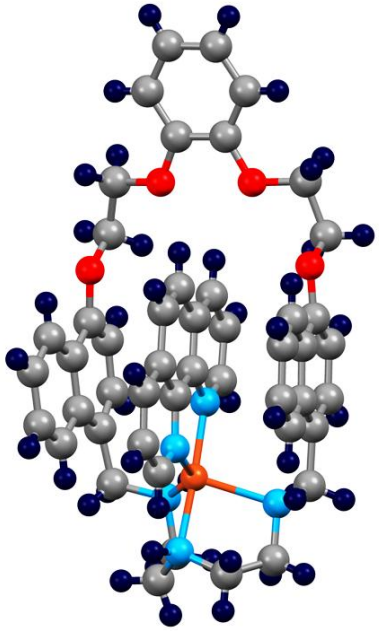

Figure 36S: Single Crystal X-ray structureof **CuPR1** (Ball and stick model).

Figure 37S: Geometry of the Cu^{II} center of **CuPR1** (τ = 0.516).

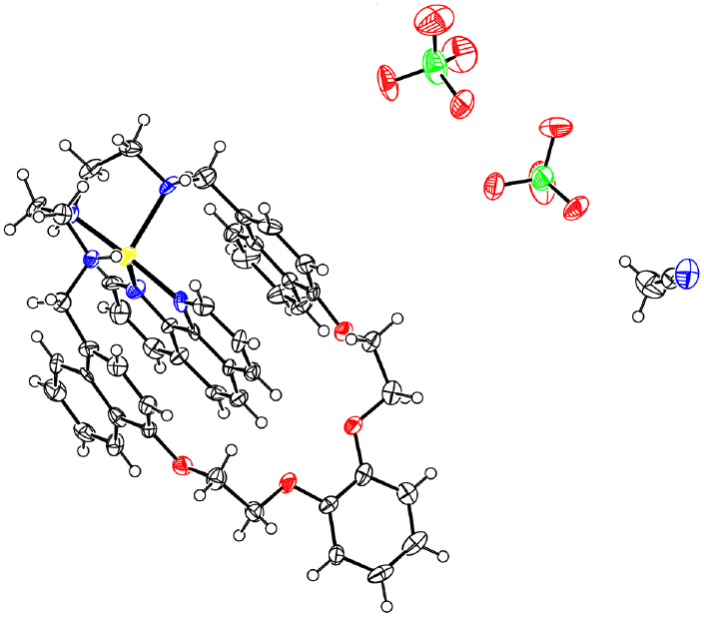

Figure 38S: Single Crystal X-ray structure of **CuPR1** (ellipsoid model using platon version).

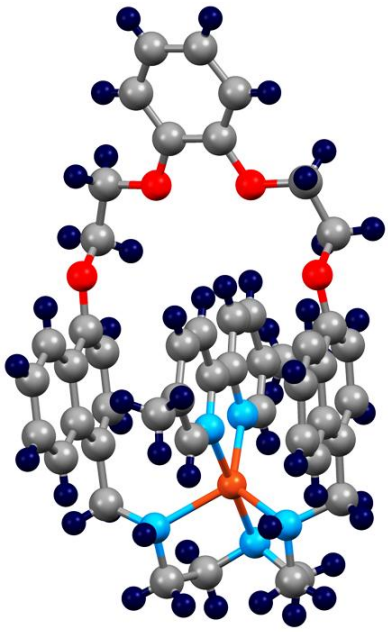

Figure 39S: Single Crystal X-ray structureof **CuPR2** (Ball and stick model).

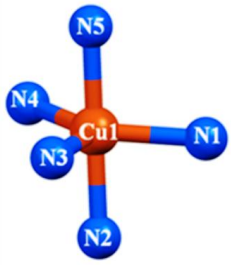

Figure 40S: Geometry of the Cu^{II} centre of **CuPR2** (τ = 0.821).

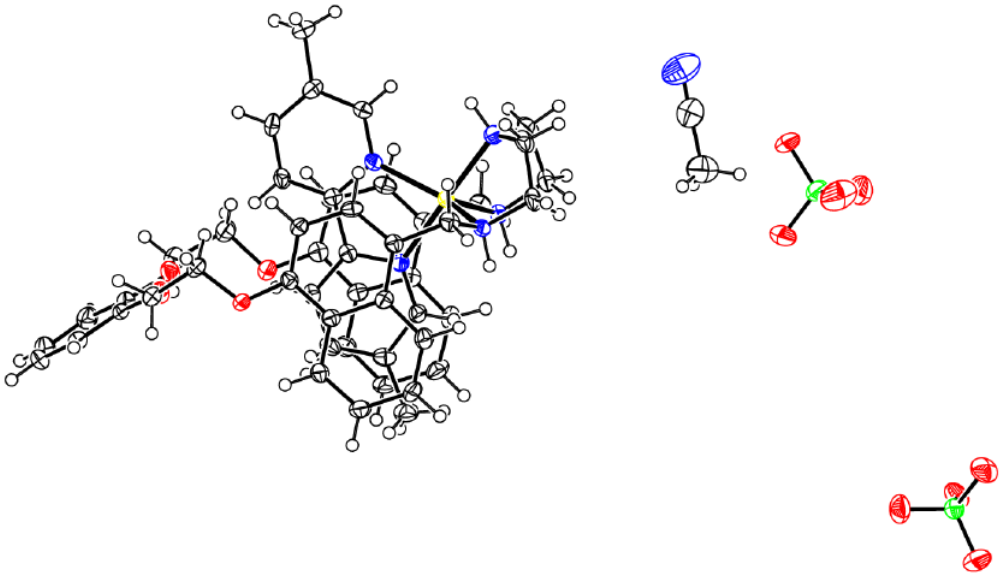

Figure 41S: Single Crystal X-ray structure of **CuPR2** (ellipsoid model using platon version).

Table 2S. N-Cu-N bond angle of **CuPR1** and **CuPR2**

CuPR1		**CuPR2**	
N1 -Cu1 -N2	**81.6(3)**	**N1 -Cu1 -N2**	**84.07(11)**
N1 -Cu1 -N3	**95.7(3)**	**N1 -Cu1 -N3**	**109.27(11)**
N1 -Cu1 -N4	**105.7(3)**	**N1 -Cu1 -N4**	**130.09(11)**
N1 -Cu1 -N5	**145.3(3)**	**N1 -Cu1 -N5**	**95.45(11)**
N2 -Cu1 -N3	**176.3(3)**	**N2 -Cu1 -N3**	**83.86(11)**
N2 -Cu1 -N4	**99.7(3)**	**N2 -Cu1 -N4**	**100.42(11)**
N2 -Cu1 -N5	**96.5(3)**	**N2 -Cu1 -N5**	**179.06(12)**
N3 -Cu1 -N4	**83.4(3)**	**N3 -Cu1 -N4**	**120.64(10)**
N3 -Cu1 -N5	**84.3(3)**	**N3 -Cu1 -N5**	**95.55(11)**
N4 -Cu1 -N5	**108.7(3)**	**N4 -Cu1 -N5**	**80.51(11)**

Table 3S. N-C-C-N torsional angle of **CuPR1** and **CuPR2**

CuPR1		**CuPR2**	
N3 -C31 -C32 -N4	**57.4(9)**	**N1 -C20 -C21 -N2**	**-48.0(4)**
N3 -C33 -C34 -N5	**-46.6(10)**	**N2 -C22 -C23 -N3**	**55.2(4)**
N1 -C41 -C42 -N2	**2.1(13)**	**N4 -C41 -C42 -N5**	**-1.8(4)**

Table 4S. Cu-N bond distance of **CuPR1** and **CuPR2**

CuPR1		**CuPR2**	
Cu1 -N1	**2.067(9)**	**Cu1 -N1**	**2.111(3)**
Cu1 -N2	**2.018(7)**	**Cu1 -N2**	**2.044(3)**
Cu1 -N3	**2.027(8)**	**Cu1 -N3**	**2.180(3)**
Cu1 -N4	**2.282(8)**	**Cu1 -N4**	**2.072(3)**
Cu1 -N5	**2.091(8)**	**Cu1 -N5**	**1.997(3)**

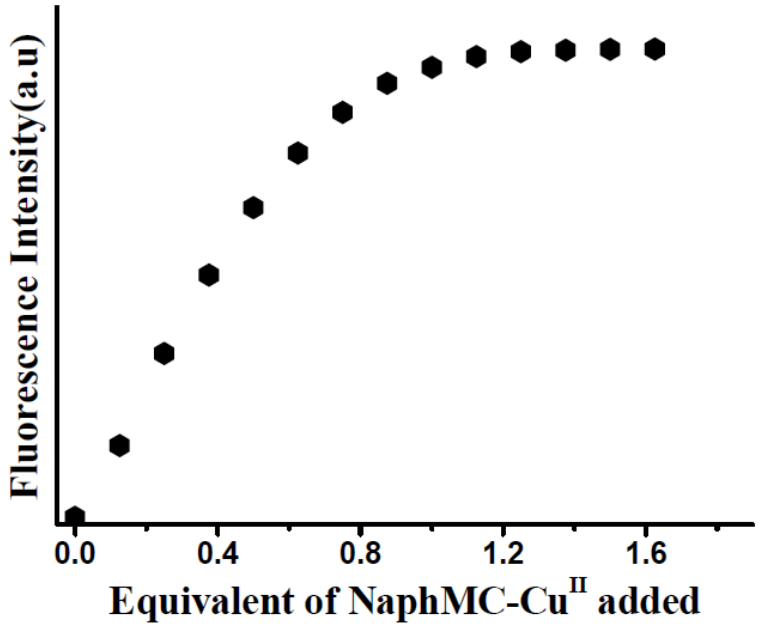

Figure 42S: Equivalence plot between **L3** and **NaphMC-Cu^{II}** (from emission titration experiment).

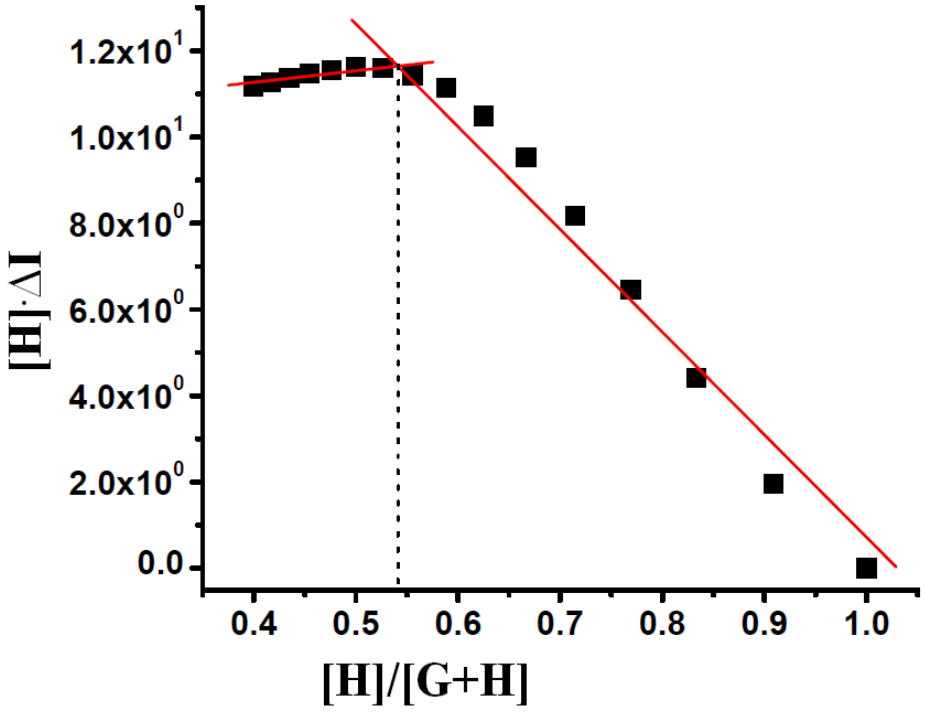

Figure 43S: Molar ratio plot of titration between **NaphMC-Cu^{II}** with **L3** (from emissiontitration experiment)**.**

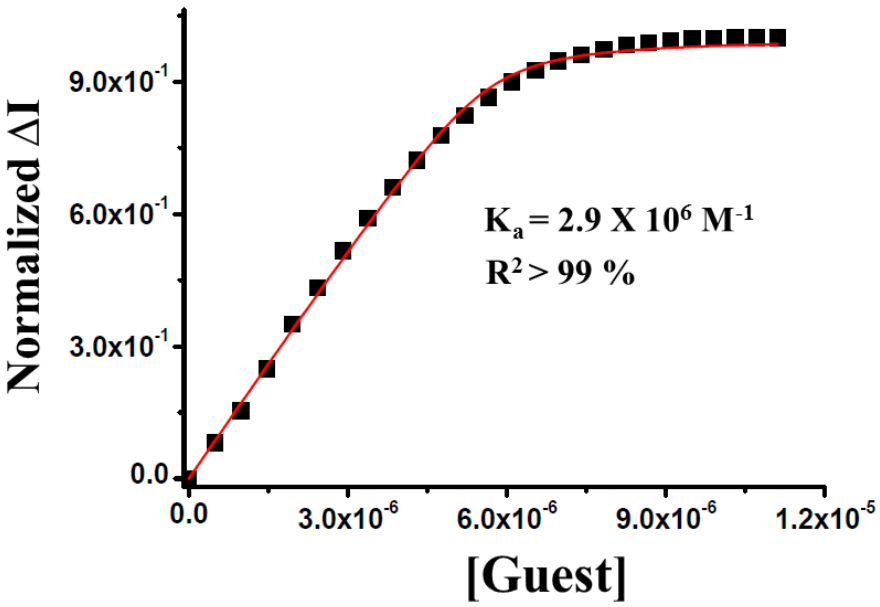

Figure 44S: Nonlinear 1:1 curve fittingplot of formation of**CuPR3** complex from emission titration experiment.

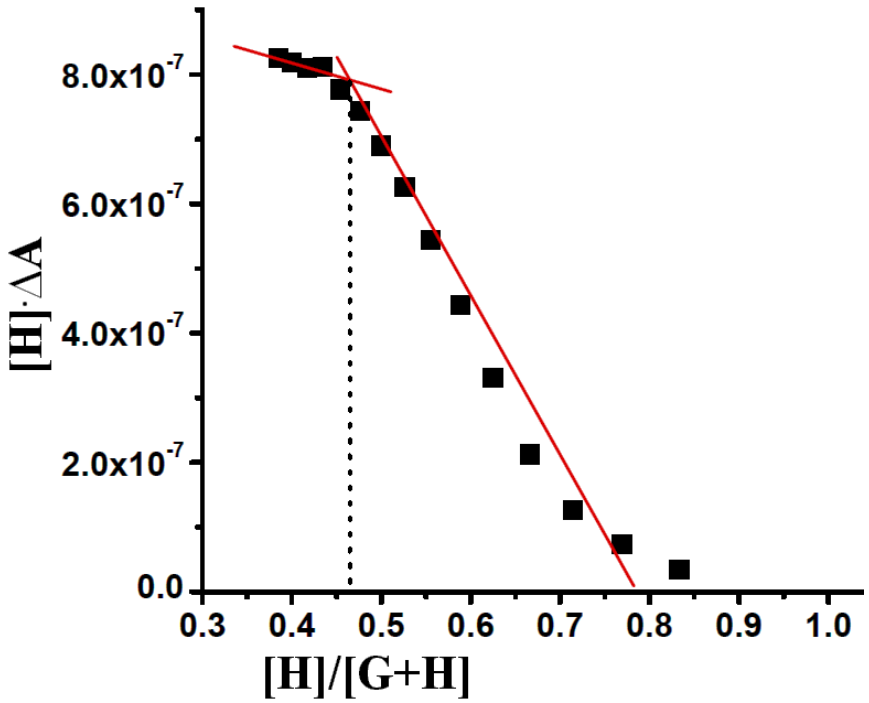

Figure 45S: Molar ratio plot of titration (UV/Vis study) between **CuPR3**with **L1.**

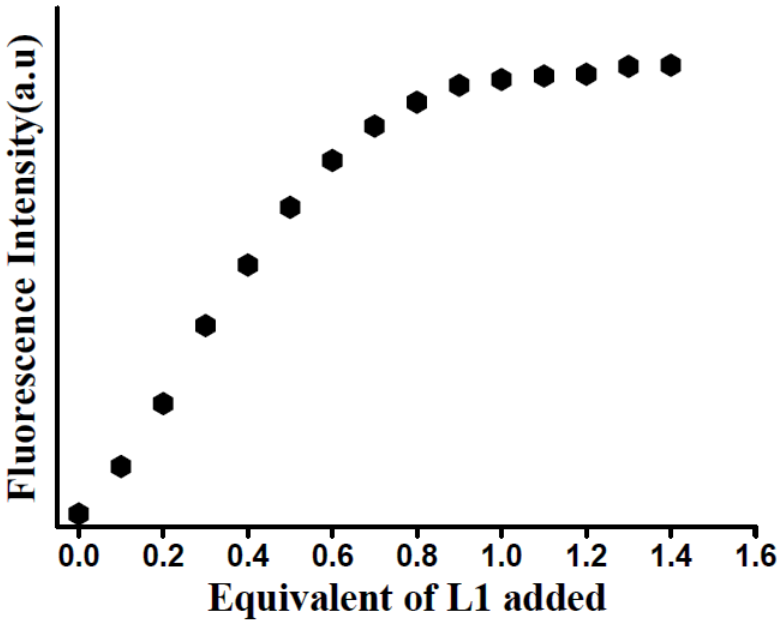

Figure 46S: Equivalence plot from emission titration experiment between **CuPR3** with **L1** in dry THF.

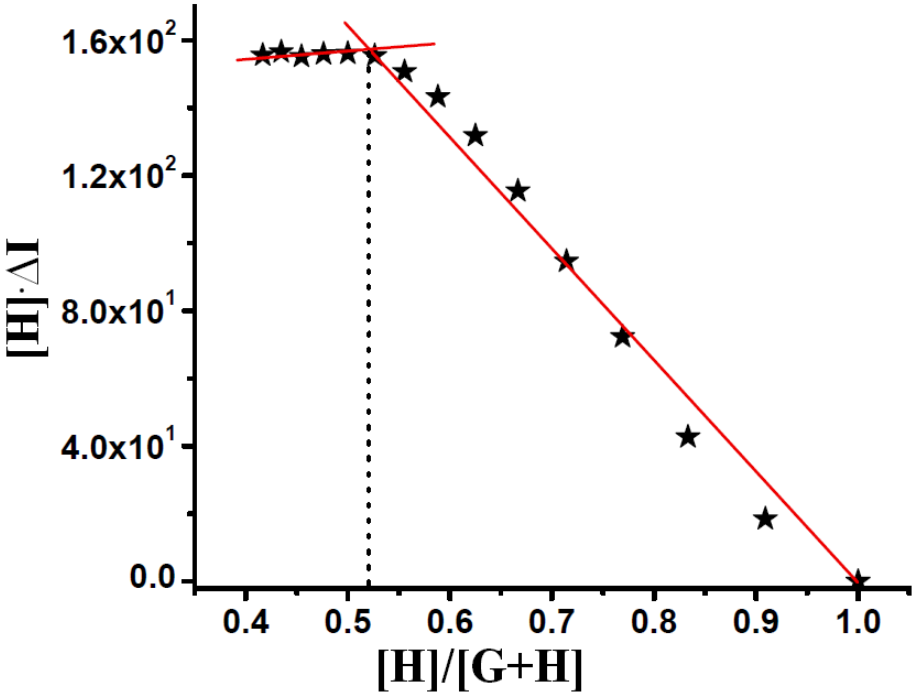

Figure 47S: Molar ratio plot of titration (PL study) between **CuPR3** with **L1.**

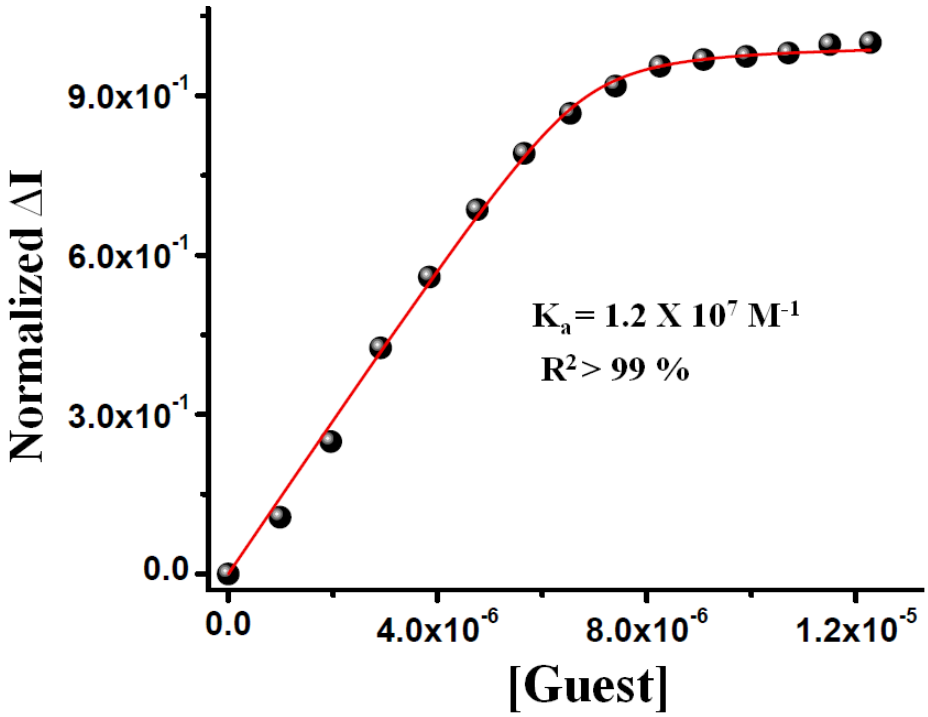

Figure 48S: Nonlinear 1:1 curve fitting from emission titration experiment between **CuPR3** with **L1** in dry THF.

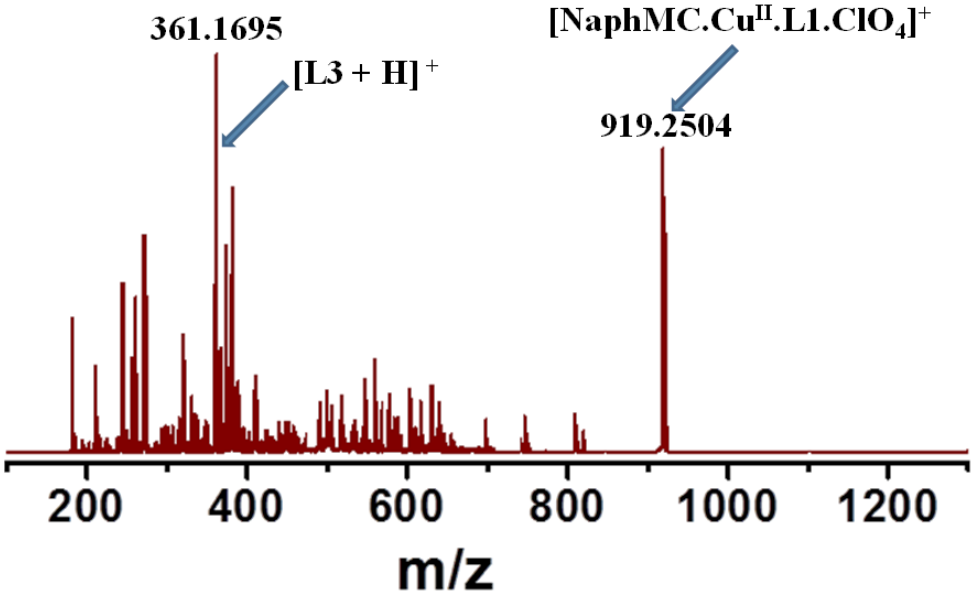

Figure 49S: ESI-MS (+ve) spectrum of resultant titrated solution from titration between **CuPR3** with **L1.**

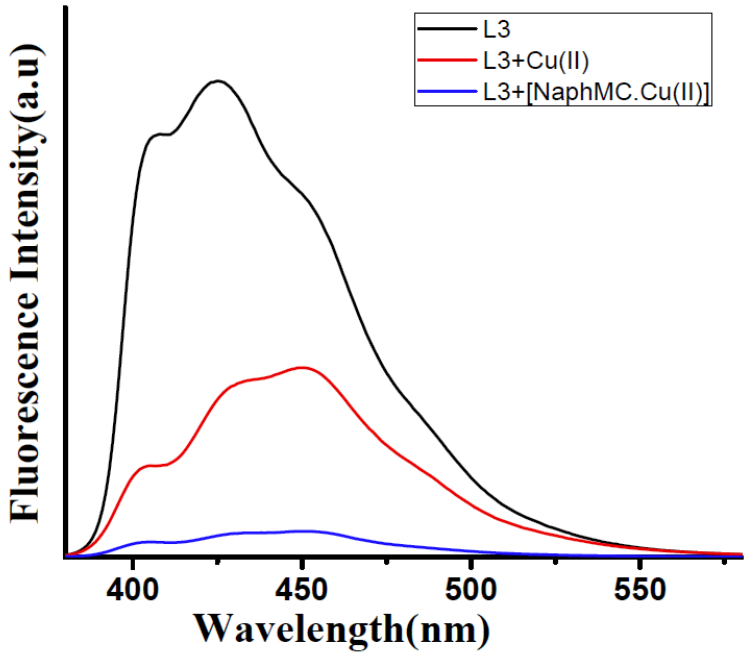

Figure50S: Comparable emission studies of **L3**, [**L3**+ Cu(II)] and [**L3**+**NaphMC**.Cu(II) complex].

REFERENCES

1. W. R. Hagen, *Dalton Trans.*, 2006, 4415–443,
2. S. Gilch, O. Meyer, I. Schmidt, *Biometals* .,2010, **23**,613–622,
3. L. Husarikova, Z. Repicka, J. Moncol, D. Valigura, M. Valko, M. Mazur., *Appl Magn Reson*, 2013, **44**,571–582.